www.amlett.com, www.amlett.org, DOI: 10.5185/amlett.2013.fdm.36 Published online by the VBRI press in 2013

Magnetic, magnetocapacitance and dielectric properties of $BiFeO_3$ nanoceramics

B. Kumari, P. R. Mandal, T. K. Nath*

Department of Physics and Meteorology, Indian Institute of Technology Kharagpur, 721302, West Bengal, India

*Corresponding author. E-mail: tnath@phy.iitkgp.ernet.in

Received: 06 January 2013, Revised: 16 March 2013 and Accepted: 01 May 2013

ABSTRACT

Single phase Bismuth ferrite ($BiFeO_3$, BFO) nanoparticles (particle size ~ 50-100 nm) were synthesized by a novel chemical sol-gel technique. The detailed microstructural analysis has been performed through HRXRD, HRTEM and FESEM techniques. The nanoparticles are found to crystallize with distorted rhombohedral structure having R3c space group. The dielectric constant and tan δ loss are found to vary monotonically with temperature measured at different frequency ranging from 1 kHz to 1 MHz. The M (H) hysteresis behavior at 5 K reveals weak ferromagnetic nature of the $BiFeO_3$ nanoparticles having coercivity (Hc) ~ 720 Oe and magnetization (Ms) ~ 1 emu/g at 5 T from SQUID measurements. The multiferroic character of BFO nanoparticles is confirmed through magnetoelectric response. The typical value of magnetodielectric response is observed to be 0.4% at 4300 Oe at room temperature at a frequency of 1 kHz. All the results suggest that the BFO nanoparticles are technologically very promising as far as magnetoelectric properties are concerned. Copyright © 2014 VBRI press.

Keywords: Dielectric behavior; ferroelectricity; weak ferromagnetism; magnetocapacitance.

B. Kumari obtained her M.Tech. degree from Indian Institute of Technology Kharagpur in Solid State Technology in the year 2013. At present she is pursuing research work for her Ph.D. degree in the Department of Physics, Indian Institute of Technology Delhi. Her research interests include magnetic, dielectric, multiferroic, nanomagnetic and optoelctronic materials for technological applications.

P.R. Mandal obtained her M.Sc. degree in Physics in 2008. She is a senior research scholar in Physics and Meteorology Department, Indian Institute of Technology, Kharagpur. Her research interests include the synthesis and characterization of structural, magnetic, dielectric, and magnetodielectric properties of different types of single and composite multiferroic materials .She is also working on nano magnetic materials.

Dr. T. K. Nath is an Associate Professor in the Dept. of Physics, Indian Institute of Technology, Kharagpur. He obtained his M.Sc. degree from Indian Institute of Technology Kharagpur in 1990 and Ph.D. degree from Indian Institute of Technology Kanpur in 1996. He was a postdoctoral fellow in Duke University, USA, North Carolina State University, USA and in Tata Institute of Fundamental Research, India. His research interests include Nanostructured magnetic materials, Magnetic thin films and multilayers, Dilute magnetic semiconductors, Superconductivity, Spintronics, Multiferroics, CMR, GMR materials, Highly spin polarized Magnetic oxides and Magnetic Huesler alloys for magnetoelectronics, Magnetocaloric materials etc.

Introduction

Multiferroic materials exhibit simultaneously more than one ferroic order parameter (ferromagnetism, ferroelectricity and ferroelasticity) in a single phase **[1]**. They have potential applications in multistate memory elements, magnetic sensors, data storage, spintronics and microelectronic devices etc. due to strong coupling between the magnetic and electric degrees of freedom **[2]**. The single phase multiferroics of ABO_3 perovskite structure at room temperature are rare because the ferroelectricity requires empty d shells and magnetism requires partially filled d shells. Among all the multiferroic materials of type ABO_3, bismuth ferrite ($BiFeO_3$ or BFO) is the most promising single phase multiferroic material exhibiting multiferrocity at room temperature from the technological applications point of view **[3]**. It has distorted rhombohedral perovskite (ABO_3) structure with R3c space group which is non-centrosymmetric. Both ferroelectricity and antiferromagnetism are present in $BiFeO_3$ single crystals. The existence of large ferroelectric polarization, as well as small magnetization is confirmed by J. Li *et al.* in case of $BiFeO_3$ thin films **[4]**. Bulk BFO contains G type – antiferromagnetism with a helical order of periodicity below the Neel temperature T_N ~ 643 K and ferroelectricity below Curie temperature T_C ~ 1103 K **[1, 5]**. The

antiferromagnetism in bulk BFO arises due to the antisymmetric Dzyaloshinskii-Moriya (DM) exchange of Fe-O-Fe bond and the hybridization between the Bi 6p and O 2p oribitals due to $6s^2$ loan pair of Bi cation causes the ferroelectricity in BFO. **[6]** The magnetoelectric interactions in bulk $BiFeO_3$ are weak because of its antiferromagnetic G-type structure. The G-type antiferromagnetic structure is long range modulated such as it is manifested in a cycloidal spiral of the length of 620 Å with the [l 1 0] spiral direction and (1 1 0) spin rotation plane **[7]**. The bulk $BiFeO_3$ suffers from poor magnetization due to its antiferromagnetic nature and modulated spin spiral structure which restrict mutiferroic property **[8]**. However, its potential applications are affected by the leakage current which arises due to impurities, defects or nonstoichiometry. Nanoscale materials, which are of great fundamental and technological interests, exhibit a wide range of magnetic, electrical, and optical properties as a result of their low dimensionality and quantum confinement effect. In this work we have reported the noticeably high magnetization for nanoscale $BiFeO_3$ (average grain size ~ 80 nm) at room temperature synthesized by chemical sol-gel method. The decrease in particle size of BFO below the periodicity of the helical order may cause the suppression of the helical order, which gives rise to the higher magnetization in nanocrystalline $BiFeO_3$. **[9]** Using the first-principles density functional theory the coupling possibility between the ferroelectric polarization and the weak ferromagnetism has been investigated [8]. The magnetoelectric coefficient of 7 mV/cm Oe at a bias magnetic field of H=120 Oe was observed by J. M. Caicedo *et al.* [10]. In this work we have investigated in details the microstructure, dielectric, magnetic, ferroelectric, magnetocapacitance $[(\varepsilon'(H) - \varepsilon'(0))/\varepsilon'(0)]$ properties and impedance spectroscopy of chemically synthesized $BiFeO_3$ (BFO) nanoparticles.

Experimental

Nano particles of BFO were prepared by a novel chemical sol-gel method using metal nitrate in 1:1 molar ratio. Bi $(NO_3)_3.5H_2O$ [99 %, Merck] and Fe $(NO_3)_3.9H_2O$ [99%, Merck] were dissolved in appropriate amount of HNO_3 and deionized water, respectively. All the two solutions are mixed into a beaker and citric acid which works as a chelating agent was added in 1:1 molar ratio with the metal nitrates with constant stirring at 70°C for 24 hrs. At the end combustion takes place and black powder is formed. The final powder was calcined at 450°C, 500°C, 550°C, 600°C for 3 hrs. The formation of proper phase was identified by a HRXRD system (Panalytical, PW 3040/60) using Cu-K_α radiation (λ = 1.542 Å). Pure phase of BFO was obtained at 500°C. Then the pellet was made using PVA as a binder and sintered at 500°C for 5 hrs to carry out its electrical and magnetic measurements. For electrical measurements silver paste was coated uniformly on both side of each pellet for excellent contact. The structural analysis of the sample has been done from the recorded XRD pattern. The surface morphology and microstructure of the sample are observed using a field emission scanning electron microscopy (FESEM) and high resolution tunneling electron microscopy (HRTEM). The dielectric constant and the impedance spectroscopy have been measured with a high precision LCR meter (HIOKI 3532-50). The magnetizations measurements of the sample are carried out using a SQUID magnetometer (Quantum Design, USA) in the temperature range from 5 - 380 K up to a magnetic field of ± 5 T.

Results and discussion

Structural analysis

Fig. 1 (a) shows the XRD pattern of the BFO nanoparticles. The XRD pattern reveals that the peaks correspond to the reflections from (012), (104), (110), (006), (202), (024), (116), (122), (018), and (300) planes of rhombohedral $BiFeO_3$ nanoparticles. We have performed Rietveld refinement of the recorded XRD pattern at room temperature with the aid of Maud program. Refinements were carried out based on hexagonal representation of space group R3c.

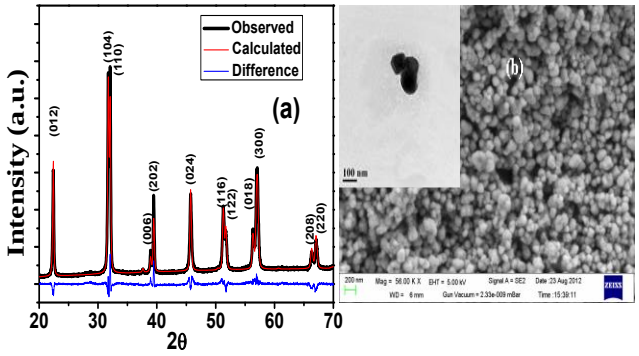

Fig. 1. (a) XRD pattern of BFO nanoparticles. **(b)** FESEM micrograph of BFO nanoparticles. Inset shows the HRTEM micrograph.

Based on the detailed Rietveld refinement on the fitting parameters (small values of R_{wp}, R_p, as listed in **Table 1**), it is concluded that the structures fit very well to the rhombohedral crystal for the sample. The FESEM micrograph of BFO nanoparticles is shown in **Fig. 1 (b)**. The inset of Fig. 1(b) shows the HRTEM image of the sample. From both micrographs it is observed that the average particle size is around 80-90 nm. The estimated lattice constant a is 5.582 Å and c is 13.877 Å at room temperature. No impurity phase has been found in the XRD pattern.

Table 1. The fitted parameters obtained from Rietveld refinement.

a(Å)	5.582
c(Å)	13.877
R_{wp}(%)	7.587
R_p(%)	5.811
Microstrain (%)	0.00123

Magnetic study

Fig. 2(a) shows the nature of magnetic hysteresis M (H) loop of BFO nanoparticles at 5 K and the inset of **Fig. 2(a)** shows magnetic hysteresis loop at room temperature (300 K).

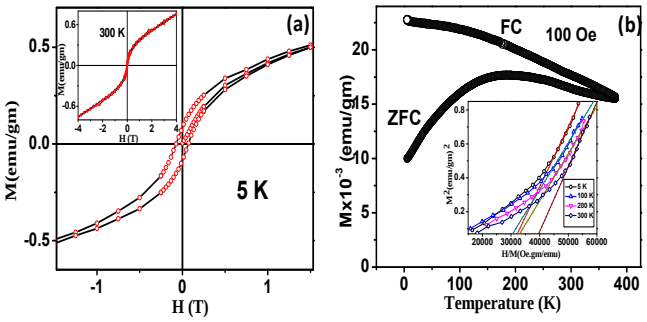

Fig. 2 (a) M-H loop of nano BFO at 5 K [inset shows M-H loop at 300 K] and **(b)** M-T curves for BFO measured at 100 Oe under FC and ZFC condition. Inset shows the Arrott plots at various temperatures.

For bulk BFO the hysteresis loop is generally observed to be linear, indicating antiferromagnetic ordering of spins at the ground state (5 K). But here the hysteresis loop is similar to a typical non-saturating weak ferromagnetic S-shaped like curve having both coercivity and remanent magnetization. The complete saturation of magnetization of these BFO nanoparticles is not achieved, even up to a applied magnetic field of 5 T (not shown here). The highest magnetization observed at 5 K at a magnetic field of 5 T is ~ 1 emu/g. The observed coercivity and remanent magnetization for the nanoparticles are H_c = 720, 355, 186, 123, 115 Oe and M_r = 0.09, 0.05, 0.03, 0.02, 0.01 emu/g at temperatures T = 5, 50, 100, 200 and 300 K, respectively. **Fig. 2(b)** shows the dc magnetization (M) – temperature (T) curve under field cooled (FC) and zero field cooled (ZFC) conditions in the temperature range of 5 to 380 K in presence of 100 Oe field. The ZFC curve shows a peak near a glass-like transition temperature, T_g ~ 175 K. There is a strong irreversibility between ZFC and FC curves starting much before the T_g, where the peak in the ZFC curve is observed. This suggests about the possibility of formation of spin cluster-glass-like phase in low temperature regime in these BFO nanoparticles. The irreversibility observed at low temperature may be correspond to the behavior of superparamgenetic, spin glass, cluster glass like phases or a weak ferromagnetic ordering as reported by Shen et al. **[11]** The existence of ferromagnetic order in the BFO nanoparticles is verified by the Arrott-Belov-Kouvel (ABK) plots which are the plots of square of magnetization (M^2) versus H/M [shown in the inset of **Fig. 2(b)**] in isothermal condition. The plots can be fitted by a linear function. The slope of the linear fit is positive and highest at 5 K. The Arrott plots show the presence of weak ferromagnetism in the BFO nanoparticles. The origin of weak ferromagnetism in the nanoparticles possibly is due to the canting of the spins mainly because of the fact that when particle size decreases, number of surface asymmetry atoms increases. Due to this, the angle of the helical ordered spin arrangement is changed and hence net magnetic moment appears **[8]**.

Complex impedance spectroscopy

The Nyquist plot i.e. the plot between real and imaginary part of complex impedance [Z^* (ω, T) = $Z' + i\,Z''$] spectroscopy of BFO nanoparticles at different temperatures has been generated from Z' (ω) and Z'' (ω) plots at wide range of frequencies and at various temperatures as shown in **Fig. 3(a)**. All the semicircles exhibit some degrees of depression indicating that the center of these semicircles lies below the abscissa axis showing presence of non-Debye type of relaxation phenomena in the material. The depressed semicircle is due to appearance of second semicircular arc which reveals the statistical distribution of relaxation times. The inset of **Fig. 3(b)** shows Z' vs. frequency plot of nanometric BFO at different temperatures. Z' decreases with increasing temperature and increasing frequency. This indicates that the conductivity increases with increasing temperature and frequency. From Z" vs. frequency plot [shown in **Fig. 3(b)**] it is clear that the Z" peak is shifted to higher frequency with increasing temperature, indicating that the relaxation rate for this process increases with rising temperature.

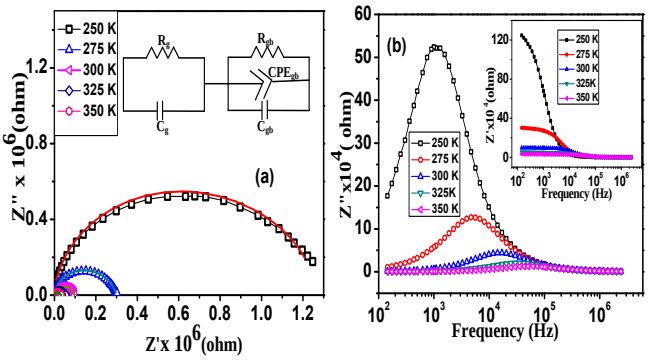

Fig. 3 (a) Nyquist plots of BFO nanoparticles. Inset shows the equivalent circuit. **(b)** Z" vs. frequency plots. Inset shows Z' vs. frequency plots.

The impedance spectra has been analyzed by fitting with an equivalent circuit consisting of a parallel combination of grain resistance (R_g) and grain capacitance (C_g) connected in series with a parallel combination of grain boundary resistance (R_{gb}), grain boundary constant phase elements (CPE_{gb}), and grain boundary capacitance (C_{gb}). The grain and grain boundary resistance and capacitances have been calculated using the fitted parameters as summarized in **Table 2**.

Table 2. The grain and grain boundary resistance and capacitance of BFO.

T (°C)	R_g×10⁴ (ohm)	C_g×10⁻¹⁰ (F)	R_{gb}×10⁴ (ohm)	C_{gb}×10⁻¹⁰ (F)	CPE_{gb} ×10⁻¹⁰(F)	n
250	19.10	19.5	107	0.79	2.07×10^{-10}	0.82
275	10.90	2.52	19.10	1.18	2.07×10^{-9}	0.69
300	0.35	1.55	6.20	1.72	7.47×10^{-9}	0.64
350	0.13	1.91	1.95	1.50	5×10^{-7}	0.39

Decrease of both R_g and R_{gb} with increase in temperature suggests an increase in conductivity with

temperature. The value of n is lower than 1, indicates the non-Debye type behavior of the sample. The bulk resistance of the sample is very high confirming insulating nature of the material. The activation energy of the BFO nanoparticles has been calculated using the Arrhenius relation, $\tau=\tau_0 \exp(-E_a/K_BT)$ where E_a is the activation energy, τ is the relaxation time. The value of the activation energy from the best fit using the Arrhenius relation is obtained to be 1.2 eV [shown in **Fig. 4**].

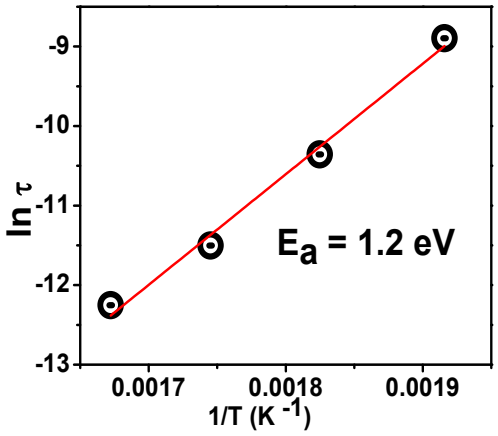

Fig. 4. Relaxation time vs. temperature.

Dielectric study

Fig. 5(a) shows the dielectric constant and dielectric loss vs. frequency plot of BFO naoparticles at room temperature. The dielectric constant of the sample decreases with increasing frequency. This indicates the dispersion due to Maxwell-Wagner type interfacial polarization which is in good agreement with Koop's phenomenological theory **[12]**.

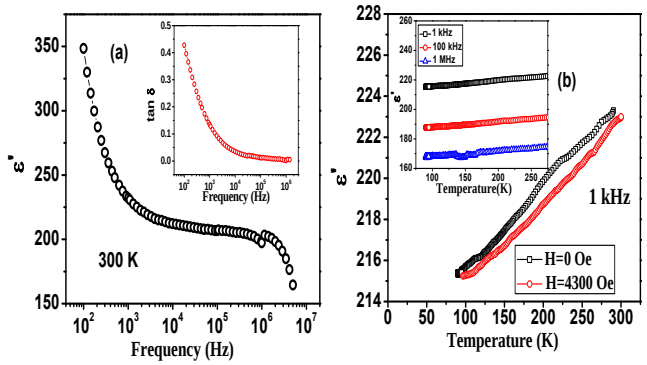

Fig. 5 (a). Dielectric constant and dielectric loss [inset of Fig. 5 (a)] vs. frequency of BFO at room temperature. **(b)** Dielectric constant vs. temperature with 4300 Oe and without field. Inset shows dielectric constant vs. temperature plots at different frequencies.

At low frequency the dielectric constant depends upon different type of polarizations, i.e. interfacial, ionic, electronic, atomic polarization. But at high frequency only electronic polarization is responsible for the dielectric constant. So there is a sharp decrease in dielectric constant at low frequency. The value of dielectric constant at room temperature at a frequency of 100 Hz is observed to be 350. The dielectric loss (tan δ) is observed to decrease with frequency. The tan δ loss decreases from 0.42 to 0.003 when the frequency increases from 50 Hz to 1 MHz. The temperature-dependent dielectric constant (ε') and dielectric loss (tan δ) were measured in the temperature range of 77-300 K for the $BiFeO_3$ ceramic sample at 1 kHz, 100 kHz, 1 MHz frequency as shown in the inset **Fig. 5 (b)**.

The dielectric constant is observed to increase with increasing temperature. **Fig. 5(b)** shows the dielectric constant vs. temperature with an applied magnetic field of 4300 Oe and without any field at a frequency of 1 kHz. This magnetoelectric effect (ME) is generally represented by the relation, $[\varepsilon(H) - \varepsilon(0)]/\varepsilon(0)$ %. We obtain the ME response of 0.4% at a frequency of 1 kHz by applying the dc magnetic field of 4300 Oe at room temperature.

The BFO nanoparticles show typical ferroelectric polarization–field (P-E) hysteresis loop at 5 Hz measured at room temperature, indicating that BFO is spontaneously polarized as shown in **Fig. 6**.

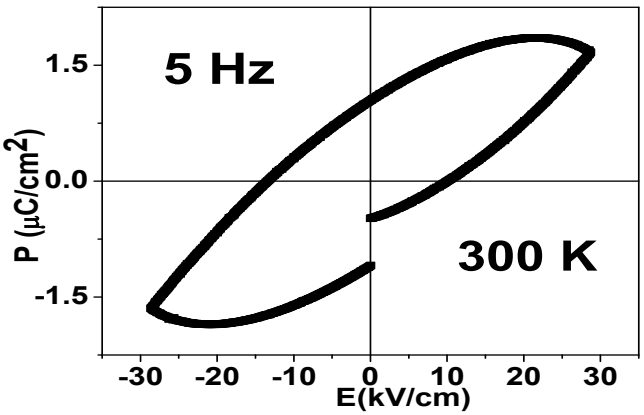

Fig.6. P-E loop of BFO nanoparticles at room temperature.

The curve is not fully saturated because of the low applied electric field. The loops indicate excellent ferroelectric behavior of the BFO nanoparticles. The coercive field (E_c) has been measured to be 12 kV/cm. We have obtained a reasonably high remanent polarization (P_r) of 1.07 μC/ cm^2. The polarization observed at highest measuring electric field of 3.4 kV is ~ 1.7 μC/ cm^2

Conclusion

In summary, we have investigated in details the microstructural, magnetic, electrical and magnetocapacitance properties of pure BFO nanoparticles (average particle size ~ 80 nm) synthesised by novel chemical citrate sol gel route. Phase purity of the synthesized nanoparticles is confirmed from the HRXRD pattern. We have observed weak ferromagnetism in the BFO nanoparticles at room temperature due to the surface-spin canting through their size confinement effect. Coercivity, remanent magnetization and magnetization of these nanoparticles are found to increase appreciably with decreasing temperature. The observation of strong irreversibility between ZFC and FC curve and a broad peak in the ZFC curve at low temperature (T_g ~ 175 K) show a glass-like transition in these nanoparticles. Impedance spectroscopy shows the non-Debye type relaxation

behavior of the BFO nano particles. Appreciable change of dielectric constant with magnetic field reveals the presence of magnetoelectric coupling in these nanoparticles. Observed ferromagnetic M-H loop, ferroelectric P-E loop and significant magnetocapacitance at room temperature in the nanometric form make this material very useful in comparison with its bulk counterpart for technologically potential device applications.

References

1. Wang D. H., Goh W. C., Ning M., and Ong C. K. *Appl. Phys. Lett.*, 2006, *88*, 212907. DOI: 10.1063/1.2208266
2. Scott J.F., *Nature Mater.*, 2007, *6*, 256 . **DOI:** 10.1038/nmat1868
3. Wang J., Zheng H., Ma Z., Prasertchoung S., Wuttig M., Droopad R., Yu J., Eisenbeiser K., and Ramesh R., *Appl. Phys. Lett.*, 2004, *85*, 2574. **DOI:** 10.1063/1.1799234
4. Li J., Wang J., Wuttig M., Ramess R., Wang N., Ruette B., PyatakovA. P., ZvezdinA. K., and Viehland D., *Appl. Phys. Lett.*, 2004, *84*, 5261 **DOI:** 10.1063/1.1764944
5. Ramachandran B., Dixit A., Naik R., Lawes G. and Rao Ramachandra S. M., *J. Appl. Phys.* , 2012, *111*, 023910. **DOI:** 10.1063/1.3678449
6. Sosnowska I, Neumaier T. P., Steichele E., *J Phys C: Solid State Phys.*, 1982, *15*, 4835-4846. **DOI:**10.1088/0022-3719/15/23/020
7. Sosnowskaa I., Loewenhaupt M., David W.I.F. and Ibberson R.M. *Physica B*, 1992, *180 & 181*, 117-118. **DOI:** 10.1016/0921-4526(92)90678-L
8. Ederer C. and Spaldin N. A., *Phys. Rev. B*, 2005, *71*, 060401. **DOI:** 10.1103/PhysRevB.71.060401
9. Park T. J., Papaefthymiou G. C., Viescas A. J., Moodenbaugh A. R., and Wong S. S., *Nano Lett.*,2007, *7*, 766. **DOI:** 10.1021/nl063039w
10. Caicedo J. M., Zapata J. A., Gómez M. E., and Prieto P., *J Appl Phys*., 1999, *85*, 4110-4119. **DOI:** 10.1063/1.2839276
11. Shen T.D., Schwarz R.B., Thompson J.D., *J Appl Phys*., 1999, *85*, 4110-4119. **DOI:** 10.1063/1.370319
12. Koops C. G., *Phys. Rev.*, 1951, *83*, 121. **DOI:** 10.1103/PhysRev.83.121